Toxicology in Vitro 85 (2022) 105473

Contents lists available at ScienceDirect

Toxicology in Vitro

journal homepage: www.elsevier.com/locate/toxinvit

Assessing the transferability and reproducibility of 3D *in vitro* liver models from primary human multi-cellular microtissues to cell-line based HepG2 spheroids

Samantha V. Llewellyn [a], Ali Kermanizadeh [b], Victor Ude [c], Nicklas Raun Jacobsen [d], Gillian E. Conway [a], Ume-Kulsoom Shah [a], Marije Niemeijer [e], Martijn J. Moné [e], Bob van de Water [e], Shambhu Roy [f], Wolfgang Moritz [g], Vicki Stone [c], Gareth J.S. Jenkins [a], Shareen H. Doak [a,*]

[a] *In vitro Toxicology Group, Institute of Life Sciences, Swansea University Medical School, Swansea University, Singleton Park, Swansea, SA2 8PP, Wales, UK*
[b] *University of Derby, School of Human Sciences, Derby DE22 1GB, UK*
[c] *Heriot Watt University, School of Engineering and Physical Sciences, Nano Safety Research Group, Edinburgh, UK*
[d] *National Research Centre for the Working Environment (NRCWE), Lersø Parkallé 105, DK-2100 Copenhagen, Denmark*
[e] *Division of Drug Discovery and Safety, Leiden Academic Centre for Drug Research, Leiden University, Einsteinweg 55, Leiden 2333 CC, the Netherlands*
[f] *MilliporeSigma, 14920 Broschart Road, Rockville, MD 20850, USA*
[g] *InSphero AG, Wagistrasse 27A, Schlieren, Switzerland*

ARTICLE INFO

Editor: Dr. P Jennings

Keywords:
Inter-laboratory trial
3D liver models
Hepatotoxicity
Nanotoxicology
Genotoxicity

ABSTRACT

To reduce, replace, and refine *in vivo* testing, there is increasing emphasis on the development of more physiologically relevant *in vitro* test systems to improve the reliability of non-animal-based methods for hazard assessment. When developing new approach methodologies, it is important to standardize the protocols and demonstrate the methods can be reproduced by multiple laboratories. The aim of this study was to assess the transferability and reproducibility of two advanced *in vitro* liver models, the Primary Human multicellular microtissue liver model (PHH) and the 3D HepG2 Spheroid Model, for nanomaterial (NM) and chemical hazard assessment purposes. The PHH model inter-laboratory trial showed strong consistency across the testing sites. All laboratories evaluated cytokine release and cytotoxicity following exposure to titanium dioxide (TiO_2) and zinc oxide (ZnO) nanoparticles. No significant difference was observed in cytotoxicity or IL-8 release for the test materials. The data were reproducible with all three laboratories with control readouts within a similar range. The PHH model ZnO induced the greatest cytotoxicity response at 50.0 μg/mL and a dose-dependent increase in IL-8 release. For the 3D HepG2 spheroid model, all test sites were able to construct the model and demonstrated good concordance in IL-8 cytokine release and genotoxicity data. This trial demonstrates the successful transfer of new approach methodologies across multiple laboratories, with good reproducibility for several hazard endpoints.

1. Introduction

Over 50 years ago, the pursuit to perform more humane animal research began with the evolution of the 3Rs principles to Replace, Reduce and Refine animal testing (The 3Rs | NC3Rs, n.d). These principles have been adopted into national and international legislation and continue to drive the advancement of *in vitro* based alternatives for pharmaceutical, chemical and engineered nanomaterial (NM) hazard assessment today. The successful implementation of *in vitro* test systems into regulatory risk assessment requires reliable prediction of toxicological outcomes associated with human exposure to exogenous substances. Liver models are designed to support *in vitro* hepatotoxicity screening, as the liver is the organ often affected by adverse drug reactions, with liver injury being the principal reason for drug withdrawals (18–30%) from the market (Onakpoya et al., 2016; Siramshetty et al., 2016). There has been significant development in improved *in*

* Corresponding author.
E-mail address: S.H.Doak@swansea.ac.uk (S.H. Doak).

https://doi.org/10.1016/j.tiv.2022.105473
Received 27 July 2022; Received in revised form 2 September 2022; Accepted 8 September 2022
Available online 13 September 2022

vitro liver culture systems, spanning 3D spheroids, microtissues and organ-on-a-chip models (Lauschke et al., 2019; Lauschke et al., 2016; van Grunsven, 2017). These advanced liver culture systems more closely emulate human physiology, through the inclusion of multiple cell types, and provision of 3D structures, fluid-flow, and relevant oxygen concentrations, coupled to more human relevant exposure regimes (Llewellyn et al., 2021a).

The liver is responsible for an array of functions, including maintaining metabolic homeostasis, synthesising and storing important biological molecules, hormone regulation and the detoxification of endogenous and exogenous substances (Trefts et al., 2017). Not only is the liver the major target organ for drug metabolism, but it is also the main site for secondary NM deposition following translocation from the site of primary exposure (*e.g.* following inhalation, ingestion, injection or dermal penetration) (Kermanizadeh et al., 2015). Whilst the field has made great strides in understanding nanosafety over the last 10-years, there have been a number of nano-specific limitations, from NM characterisation and dosimetry considerations, through to *in vitro* model design and assay interference (Llewellyn et al., 2021a; Hirsch and Schildknecht, 2019; Bohmer et al., 2018; Hirsch et al., 2011). To overcome some of these issues, there has been a focus on the development of physiologically relevant advanced 3D *in vitro* liver models that demonstrate liver-like functionality, metabolic activity, and support nanosafety assessment (Llewellyn et al., 2020; Conway et al., 2020). Two such advanced liver model systems utilised in this study, have been shown to accurately detect chemicals (*e.g.* diclofenac, aflatoxin B1, benzo[*a*]pyrene (B[*a*]P)) known to elicit a toxic response, as well as support NM hazard assessment (Llewellyn et al., n.d.; Kermanizadeh et al., 2019a; Kermanizadeh et al., 2012).

The primary multi-cellular liver model is the most representative *in vitro* model for the human liver and has been deemed the 'gold standard' for *in vitro* drug metabolism and toxicology. This commercially available, scaffold-free, 3D hepatic microtissue (3D InSight™ multi-donor human liver microtissue, InSphero) composed of primary human hepatocytes, human liver-derived Kupffer cells, and sinusoidal endothelial cells has been shown to identify hepatoxic effects associated with zinc oxide (ZnO), titanium dioxide (TiO2) and cerium dioxide (CeO2) NMs during a two week, sub-lethal (0.62 μg/mL – 10.0 μg/mL) repeated exposure regime (Kermanizadeh et al., 2019a). Post exposure, the PHH microtissues were also shown to recover and emulate aspects of liver regeneration similar to that found *in vivo*. These microtissues, however, can be limited by inter-individual donor variability and the lack of actively proliferating cells required to support genotoxicity testing endpoints required for regulatory approvals, including the *In Vitro* Micronucleus Assay (OECD Test Guideline 487) (Conway et al., 2020; Sison-Young et al., 2017). An easily accessible, relatively cost-effective alternative to the PHH models, is the well characterised cell line-based 3D HepG2 spheroid model, which due to its proliferative nature can support genotoxicity testing for both chemicals and NMs (Conway et al., 2020). Llewellyn et al., established that the HepG2 model could support extended culture periods (up to 14 days) and found that the NM associated toxicological response differed in relation to the exposure duration selected (Llewellyn et al., n.d.). In addition, an NM genotoxicity potency ranking was established, based on significant micronuclei induction observed in the 3D HepG2 spheroids following acute, low-dose (0.2 μg/mL – 10.0 μg/mL) exposure to a range of NMs (TiO2, ZnO, silver (Ag), barium sulfate (BaSO4) and CeO2,) (Llewellyn et al., n.d.).

Whilst both the PHH and HepG2 *in vitro* liver models have been applied in NM hazard assessment studies investigating a variety of endpoints (Llewellyn et al., 2020; Conway et al., 2020; Llewellyn et al., n.d.; Kermanizadeh et al., 2019a; Kermanizadeh et al., 2019b; Kermanizadeh et al., 2014; Llewellyn et al., 2021b), they need to undergo validation to support their use for regulatory purposes. Therefore, this study aimed to assess the transferability and reproducibility of the primary multi-cellular liver microtissues and the 3D HepG2 liver model across both academic and industrial laboratories, by undertaking an inter-laboratory trial. To achieve this, two independent inter-laboratory trials were conducted, one for the PHH microtissue model including the host laboratory (Laboratory A) and two academic laboratories (Labs B and C); and another for the 3D HepG2 spheroid model involving the host laboratory (Laboratory I) and three other recipient laboratories (academic: Laboratory II and Laboratory III; industrial contract research organization (CRO): Laboratory IV). This trial aimed to assess the robustness of these models and their applicability for evaluating cytotoxicity, (pro-)inflammatory response and genotoxicity, following NM exposure.

2. Results

2.1. Primary multi-cellular liver microtissue model

As the multicellular liver models are produced by the manufacturer (InSphero) and shipped directly to the participating laboratories, no model optimisation was required.

2.1.1. Cytotoxicity

To assess cytotoxicity, the integrity of the cell membrane was evaluated using the presence of an intracellular phosphotransferase enzyme, adenylate kinase (AK). Following acute (24 h) exposure to TiO2 and ZnO NMs, the cellular supernatant was analyzed for the presence of AK *via* the quantification of light emitted from the sequential reaction of ATP and luciferin, catalysed by luciferase, to form light. For the multicellular liver model, the cytotoxicity data for the positive control chemical, Triton-X was consistent between all three laboratories (Fig. 1). The

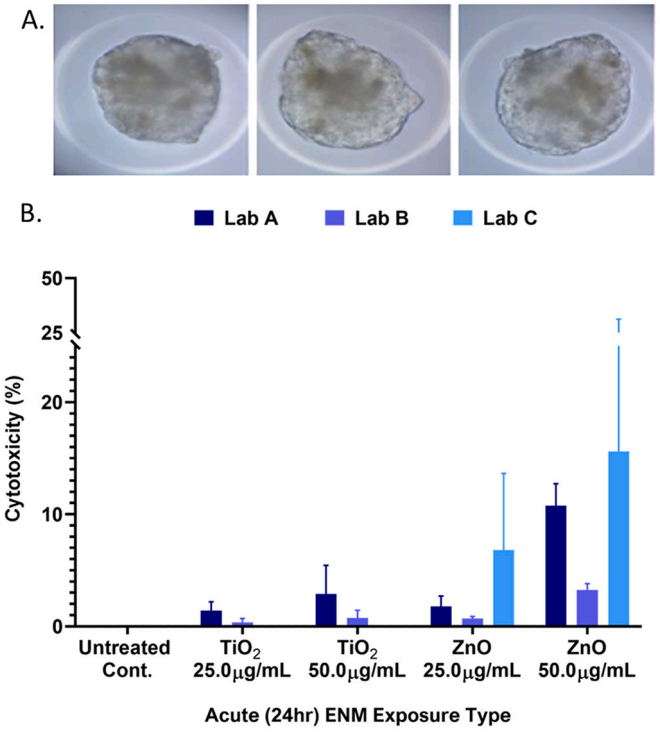

Fig. 1. (A) Light microscopy images of three representative untreated PHH microtissues. The microtissue were mounted in a custom stage on an inverted microscope (Motic, Germany). The images were acquired using a 40× air objective (Olympus, UK) using a Canon 650d camera (Canon, UK). (B) Cytotoxicity response following acute (24 h) exposure to TiO2 and ZnO NMs, across three independent academic laboratories. Untreated media only was used as the negative control whilst 1.0% Triton-X was used as the positive assay control. Mean data ($n = 3$) ± SEM is presented. Statistical significance was determined using a two-way ANOVA test with a Tukey's multiple comparisons test and is indicated as follows: * = $p < 0.05$ *vs.* untreated control.

toxicity responses to the NMs were very similar, with the ZnO exposure (50 μg/mL) showing the highest level of cytotoxicity (3.3% - 15.6%) and TiO2 exposure (25 μg/mL) showing the lowest level of cytotoxicity (0.0–1.4%) across all three laboratories. Whilst the cytotoxicity varied between laboratories, with Laboratory C data appearing consistently higher than that of the host laboratory and Laboratory B, the data trends were consistent and there was no statistically significant difference observed between the laboratories in response to individual NM exposure treatments. In addition, neither TiO2 or ZnO NMs induced a statistically significant increase in cytotoxicity, relative to the untreated negative control, in the PHH microtissue models following 24-h exposure. Diclofenac was also used as a supplementary positive control by the host laboratory, Laboratory A and Laboratory C, but not by Laboratory B due to supplier restrictions. Nonetheless, 240 μM of diclofenac was shown to induce moderate cytotoxicity (2.3–13.8%) in both laboratories respectively (data not shown).

2.1.2. IL-8 (pro-)inflammatory response

The cytokine, IL-8, is a major mediator of the inflammatory response and was selected for analysis, as it is a commonly used early-phase biomarker and is secreted by several cell types, including hepatocytes (Bishara, 2012). As a result, data in Fig. 2 is from two laboratories (Laboratory A and Laboratory B). These data show that both NMs (ZnO and TiO2) induce IL8 release from the primary liver models in a dose dependent manner, with the greatest IL-8 release after exposure to TiO2 (Laboratory A) and ZnO (Laboratory B) at the highest doses used (50 μg/mL). Despite consistency in the data between the two laboratories the observed effects were not statistically significant ($p \geq 0.05$) as a result of intra-replicate variation. Nevertheless, the graph shows clear trends for increased IL-8 cytokine release in both laboratories in a dose dependent manner for both NMs.

2.2. 3D HepG2 spheroid model

2.2.1. Model transfer and optimisation

The first step in the inter-laboratory transfer of the SOP to culture the 3D HepG2 spheroid model was to evaluate the ability of the recipient laboratory to construct the model successfully prior to initiating any *in vitro* toxicity assessment. This initial stage was largely successful, as the recipient laboratories were able to construct the 3D HepG2 spheroid models. However, there were some minor issues experienced when establishing the models, which included reduced spheroid yield and the formation of non-spherical shaped spheroids. This was resolved with some additional advice included in the SOP (Llewellyn et al., n.d.; PATROLS SOP Handbook, n.d) regarding the use of specific plasticware (*i.e.* specific Nunc™ MicroWell™ 96-Well Microplates required), cell supplier (*i.e.* ATCC HB-8065 HepG2 cells, with no >7 passages upon retrieval from liquid nitrogen), seeding technique (*i.e.* pipette angled as close to 90° from the plate as possible) and handling of the plates (*i.e.* minimise disturbance during spheroid formation) (Fig. 3).

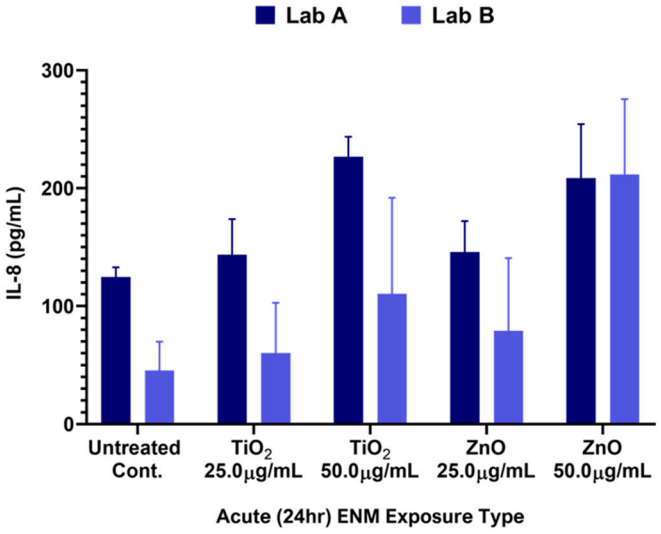

Fig. 2. IL-8 (pro-)inflammatory response in PHH microtissues, following acute (24 h) exposure to TiO2 and ZnO NMs, across two independent academic laboratories. An untreated, media only sample was used as the negative control. Mean data ($n = 3$) ± SEM is presented. Statistical significance was determined using a two-way ANOVA test with a Tukey's multiple comparisons test and is indicated as follows: * = $p < 0.05$.

Once rectified, the second attempt to construct the model was a great success, with the feedback from the other laboratories summarised in the following points:

1. "The cell viability went up in both the vehicle and untreated models (> 90%). Most spheroids have a smooth border and good spherical shape."
2. "This technique allows for the fast preparation of liver spheroids (i.e. ≤ 3 days), with no interference or batch-to-batch variation introduced from the presence of a matrix scaffold."

The 3D HepG2 spheroid model construction step was therefore successfully transferred and reproduced in three laboratories, each of which reported high yields of spheroids with good viability and compact, spherical structures (Fig. 3).

2.2.2. IL-8 (pro-)inflammatory response

In both laboratories, the TNF-α positive control induced a highly significant ($p \leq 0.0001$) IL-8 response and the standard curves all fell within a similar range, thus confirming the IL-8 ELISA was executed effectively by all participants. The TNF-α response was the only significant difference found between the two laboratories, with Laboratory II displaying a 1.78-fold increase in IL-8 release when exposed to 0.25 μg/mL of TNF-α protein in comparison to Laboratory I. Overall, there was no statistically significant difference between Laboratory I and Laboratory II in the IL-8 response observed following prolonged BaSO4 exposure, regardless of the NM exposure concentration. However, within the independent laboratory data sets, there was a notable difference in the BaSO4 concentration that induced the greatest IL-8 response relative to the untreated control (Fig. 4). Both laboratories observed an increase in IL-8 release following longer-term exposure to 0.2 μg/mL of BaSO4, as shown in Fig. 4, but only the host laboratory, Laboratory I showed a statistically significant ($p = 0.008$) increase as compared to the untreated, negative control. Although the trends in IL-8 release differed slightly between the two laboratories, this was not significant.

2.2.3. Genotoxicity response

Previously it has been demonstrated that the 3D HepG2 spheroid model can be used to evaluate genotoxicity using the CBMN assay (Llewellyn et al., 2020). This 3D model has been adapted to allow for quantification of binucleated cells containing micronuclei, following acute exposure to both chemicals and NMs. During this interlaboratory trial, the recipient laboratory was able to successfully grow the 3D HepG2 spheroid model. Following exposure to a dose range of B[*a*]P, excellent concordance was observed across the host and recipient laboratories (Table 1). The recipient laboratory, Laboratory IV, reported the first induction of micronuclei at 4.0 μM in the 3D HepG2 liver spheroids, which is in alignment with the data generated by the host laboratory, Laboratory I. This demonstrates that the lowest observed effect level (LOEL) at which the first significant induction of micronuclei was observed was the same between the two laboratories, with a similar fold-change in micronuclei (Table 1). In addition, the toxicity data between the two laboratories was also closely aligned with ≤5.52% difference in cell viability values between both laboratories and a similar dose dependent decrease in cell viability observed.

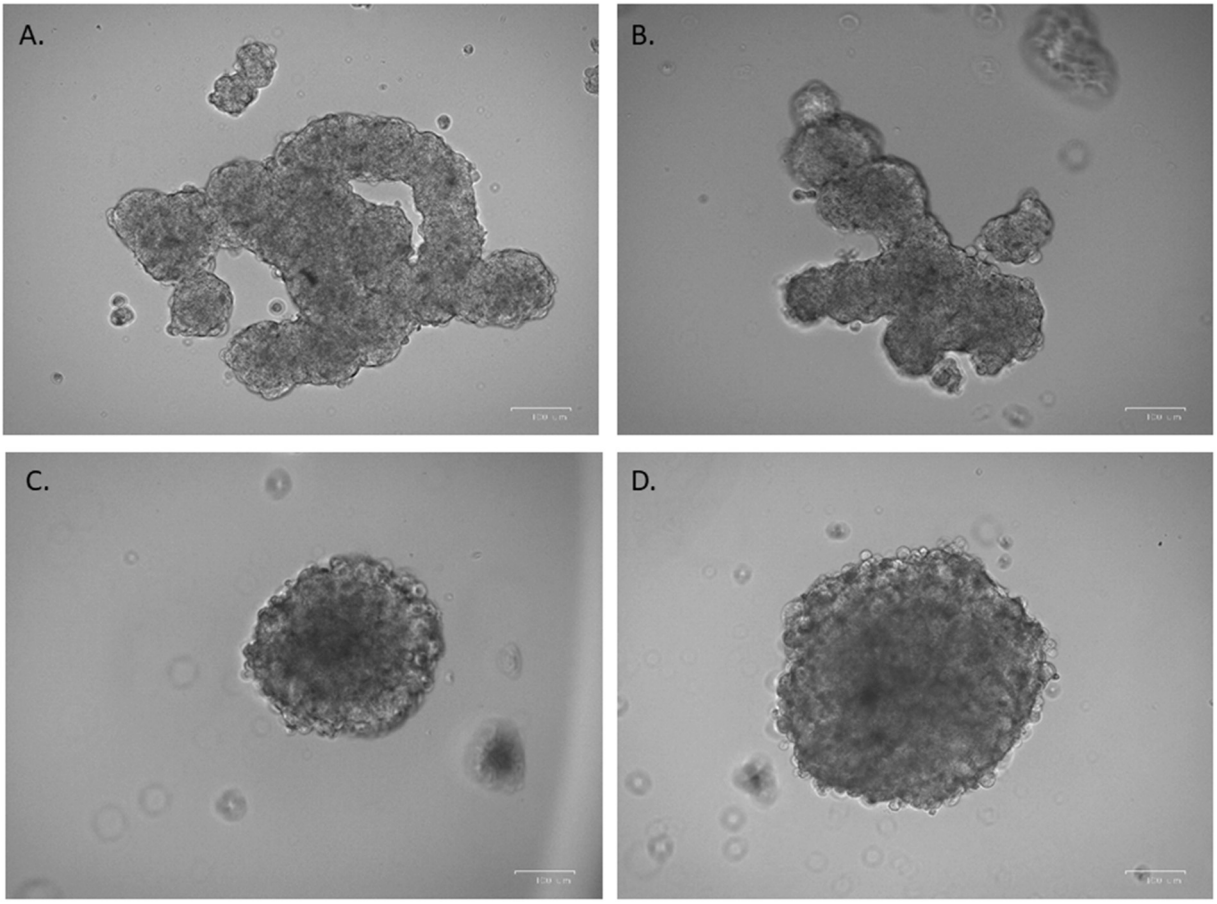

Fig. 3. Light microscopy images of HepG2 spheroid formation in the recipient laboratory, Lab III. (A-B) These images were obtained following construction of spheroids using a high passage (p18) of HepG2 cells that were seeded on Costar 96-well plates; both of which were not recommended in the initial version of the SOP. Following these issues, further detail was provided in the SOP to highlight the importance of passage number and specific use of Nucleon 96-well microplates plates as critical factors affecting spheroid formation. Images taken on a BioRad ZOE Fluorescent cell imager, using a 20× objective. Scale bar represents 100 μm. (C—D) Representative images of spheroid constructed using a low passage (p.7) of HepG2 cells and seeded on the Nucleon 96-well microplates as specified in the SOP. Images were taken at 10× objective, scale bar represents 100 μm.

3. Discussion

Interlaboratory trial experiments are a necessary step in the evaluation and validation of new approach methodologies for safety assessment purposes. As a result, the focus of this study was to assess the transferability and reproducibility of two advanced *in vitro* liver culture systems, the PHH microtissue and 3D HepG2 spheroid models, for NM hazard assessment.

3.1. Transferability of the liver models

The first challenge was ensuring that the 3D tissue models could be successfully transferred from host laboratory to the recipient laboratories, prior to evaluating their reproducibility for hazard assessment purposes. The PHH models were prepared assay-ready by commercial supplier and shipped to the recipient laboratories with limited intervention alongside previously validated SOPs detailing PHH handling protocols. The recipient laboratories that were unfamiliar with the models, adapted quickly to using the PHH microtissues and reported that no necessary changes or clarifications to the handling SOPs were required.

In contrast, the 3D HepG2 model had to be constructed by the user, therefore the quality of the 3D *In Vitro* HepG2 Spheroid Model SOP and support provided had to be transcendent. It was notable that the 3D HepG2 liver spheroid model was successfully transferred to laboratories from both academic and industrial sectors with only minor issues encountered during the model construction. Common issues raised included a reduced spheroid yield and the formation of non-spherical shaped spheroids, but they were readily resolved with additional advice that was subsequently included in the SOP, (Supplemental Information) (Llewellyn et al., 2020; PATROLS SOP Handbook, n.d). The main outcomes from this trial were the necessity for 'practice' runs, to build familiarity with the models, before the formal trial commenced. Additionally, the importance of carefully structured, clear and comprehensive SOPs with the inclusion of additional 'troubleshooting' sections, was highlighted as these were invaluable for assisting the recipient researchers to successfully reproduce the models.

3.2. Reproducibility of the toxicity data

The data from the PHH inter-laboratory trial showed great consistency with mirrored trends for the selected positive controls and NMs, with no statistically significant difference between laboratories in the cytotoxicity or IL-8 release data found. The data was largely reproducible, with all three laboratories reporting ZnO NMs to induce the greatest dose dependent cytotoxicity in the PHH model, as well as an NM associated dose-dependent response in IL-8 release. More inter-replicate variability was observed in the PHH tissues, than with the HepG2 Spheroid model, but this was to be expected due to the smaller sample size (*i.e.* the number of microtissues harvested per treatment). A previous study undertaken using the InSphero PHH co-culture microtissues were found to exhibit significant inter-donor variability (Kermanizadeh

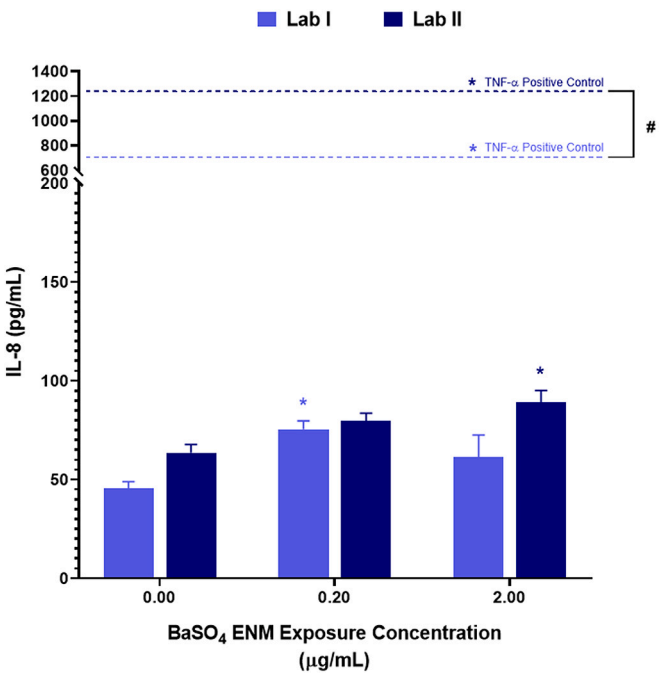

Fig. 4. (Pro-)inflammatory IL-8 response in 3D HepG2 liver spheroids, following prolonged exposure to BaSO4 NMs, across two independent academic laboratories. An untreated, media only sample was used as the negative control whilst 0.25 µg/mL of TNF-α protein (NBP2–35,076-50µg, Biotechne, UK) was used as the positive assay control. Mean data ($n = 3$) ± SEM is presented. Statistical significance was determined using a Shapiro-Wilk normality test paired with a two-way ANOVA and Tukey's multiple comparisons test and is indicated as follows: * = $p < 0.05$. Comparison between the laboratories is indicated by #, and the * demonstrates significance within independent laboratory data sets relative to the untreated negative control.

Table 1
Inter-laboratory Trial for Genotoxicity Testing with the Pro-Carcinogen Benzo[*a*]pyrene (B[*a*]P). DNA damage in HepG2 Liver Spheroids following acute (24 h) exposure to B[*a*]P across two independent laboratories. A sample of 12 HepG2 spheroids were pooled per treatment and 1000 binucleate cells were scored per replicate for the presence of MN. Mean data ($n = 3$) is presented. Statistical significance in relation to the untreated control is indicated in the table as follows: * = $p < 0.05$.

B[*a*]P Concentration (µM)		0.0	2.0	4.0	8.0
Laboratory I	Micronucleus Frequency (%)	1.60	2.17	5.03*	6.20*
	Fold-Change from Untreated Control	–	1.356	3.144	3.875
	Cell Viability (%)	100.00	95.90	93.44	90.16
Laboratory IV	Micronucleus Frequency (%)	1.10	1.10	2.70*	2.90*
	Fold-Change from Untreated Control	–	0.000	2.455	2.636
	Cell Viability (%)	100.00	97.67	96.51	95.68

et al., 2019a). Whilst the trend observed for the NM-induced biological response was very similar, the individual responses for cytotoxicity, caspase activity and cytokine (IL-6 and IL-8) secretion following exposure to a range of NMs was significantly different (Kermanizadeh et al., 2019a). To reduce the chance of variation in toxicology data arising because of different donor tissues, InSphero ensured each laboratory involved in this trial received PHH microtissues from the same donors. As a result, any inter-laboratory variation observed following the trial is likely to have arisen during the handling of the PHH microtissues, NM preparation, exposure and harvest, or the individual assays themselves. In parallel with this, the HepG2 cells utilised by each laboratory in this study were purchased specifically for the trial and were sourced from identical suppliers. Whilst this reduces the variation in cell source, it does not eradicate variation in cell counting and seeding. Elliott et al., previously found that the variability in cell densities seeded for different replicates in one laboratory alone varied by as high as 20%, whilst Niepel and colleagues found variations in MCF10A seeding densities across five independent laboratories to be the source of up to a 200-fold difference in growth inhibition rates (Niepel et al., 2019; Elliott et al., 2017). Variations in cell densities can affect the formation of the spheroids, the transport of nutrients and waste between the cells, and the cell viability. For example, the more compact a spheroid is due to higher cell numbers, the greater the levels of hypoxia in the core of the spheroid and subsequently, the greater the cell death and IL-8 release observed (Shah et al., 2018; Desbaillets et al., 1997; Sonna et al., 2003). As a result, variations in HepG2 cell densities could have been responsible for the slightly elevated IL-8 response observed in the untreated control reported by Laboratory II. Although the different IL-8 response observed between two different concentrations of BaSO4 are more likely to be due to NM preparation, dispersion and exposure or ELISA variation as mentioned previously.

For each experiment, an identical plate plan was followed by each laboratory and the microtissues located in the outermost wells of the 96-well plates were not included to circumvent the so-called "edge effects" that occur during longer incubation times of cells seeded in small volumes (*i.e.*, evaporation) (Elliott et al., 2017). Each laboratory used NMs sourced from the JRC and conducted the NM preparation and exposure, in parallel, following the same NM dispersion SOP (Alstrup Jensen, 2014), on the same day for all three biological replicates. This was important as NMs alone introduce additional variability due to the more complex nature of their physico-chemical characteristics and subsequent interaction with the biological environment (*e.g.* agglomeration, precipitation and dissolution properties). Without a predefined NM dispersion protocol, with a specified timeframe between dispersion and dosing, differences in NM protein corona formation, particle agglomeration and sedimentation can arise; all of which can introduce variation in NM exposure concentrations and particle-cell interaction (Elliott et al., 2017; Petersen et al., 2020). Following acute exposure, the supernatants were harvested and pooled from 8 PHH microtissues. A small volume of supernatant was utilised to run the AK cytotoxicity assay immediately, as stated in the manufacturer's instructions, whilst the remaining supernatant was frozen at −80 °C for IL-8 ELISA analysis at a later date. Even with a stringent SOP, followed simultaneously by all participating laboratories, there will always be slight differences in the NM stocks, reagents, endpoint kits, equipment availability and set-up, as well as the technical ability and processing speed of the individual researchers. These inconsistencies may have contributed to the observed differences in the IL-8 inflammatory response found in both the PHH and HepG2 trials. Although the trends in IL-8 response between the laboratories were similar, the variations in raw data lead to marginally differing outcomes. The greatest IL-8 response in Laboratory I and Laboratory II's HepG2 models arose following prolonged exposure to different concentrations of BaSO4. Another source of variation could have been the endpoint assay itself, as a result of the numerous wash steps in an ELISA (manual or automated) and different quality of reagents / antibodies, to enzyme-substrate reaction time and plate readers (Petersen et al., 2020). Previous inter-laboratory trials have found varying degrees of alignment in ELISA derived cytokine data, with one trial reporting mixed results of IL-1β or TNF-α release following Ag NM exposure, and other trials illustrating similar trends in cytokine release across the participating laboratories, but the exact degree of cytokine release varied significantly between the laboratories (Xia et al., 2013; Piret et al., 2017; Barosova et al., 2021). All laboratories used IL-8 ELISA kits from the same manufacturer, but the IL-8 kits utilised had different lot numbers and were accompanied with different ELISA plates (*e.g.* half area *vs* full area plates) and plate readers. Our findings support that an ELISA can potentially yield a qualitative interlaboratory agreement, but

further refinement of the assay protocols is required to yield a quantitative agreement. Therefore, to improve data consistency in the future, it is suggested that either all the supernatant samples are taken from the participating laboratories and sent back to the host laboratories for endpoint analysis, or regents purchased by a single laboratory and distributed to others participating in the inter-laboratory trial.

For genotoxicity testing utilising the *in vitro* micronucleus assay, it was encouraging that the recipient laboratory was able to replicate data generated by the host laboratory, with a matching LOAEL of 4.0 μM B[*a*]P. Previously, it has been demonstrated that HepG2 cells exhibited a higher induction of micronuclei at a lower dose of B[*a*]P in the 3D model than when they were grown in 2D (Conway et al., 2020; Shah et al., 2018). This data was highly encouraging, demonstrating excellent transfer of the 3D HepG2 spheroid model to another laboratory and highlights the importance of standardized protocols for general cell practice and accompanying endpoint assays (Hirsch and Schildknecht, 2019).

3.3. Future recommendations

The present inter-laboratory trial has demonstrated that both the PHH microtissue and 3D HepG2 liver spheroid models were successfully transferred to at least two different laboratories, including both academic and industrial sectors. The trial assessed at least two different hazard endpoints, a feature previously recommended by Xia et al., as well as a positive chemical control and at least one NM for each model (Xia et al., 2013). This pre-validation inter-lab transferability and reproducibility study confirmed the efficacy of these advanced *in vitro* 3D models for NM and chemical hazard assessment. The next steps in order for these models to be considered as part of the battery of standardized *in vitro* tools for regulatory NM assessment, is to conduct a larger-scale round-robin approach with a greater number of chemicals and NMs and laboratories. A significant advantage of conducting this inter-laboratory trial was the advanced development of the SOPs required to set-up and apply the two 3D *in vitro* liver models successfully. These SOPs have now been tried and tested and form a strong foundation for future validation trials (https://patrols-h2020.eu/publications/sops/index.php.). Based on this study, our recommendations to be considered when designing an inter-laboratory trial to assess the transferability and reproducibility of an *in vitro* model, would be to:

- Construct robust and detailed methodology following GIVIMP guidance (OECD, 2018), which highlights the importance of fulfilling the exact requirements set out by the SOP (*e.g.*, cell sources, plasticware, dispersion protocols).
- Ensure personnel are trained in person on the use of the models and different endpoints being carried out. This was not possible for this study, due to impact of COVID-19 on travel and lab closures. However, alternative tools were utilised such as video recordings and webinars.
- Ensure that the *in vitro* model is fully characterised using physiologically relevant and functional endpoints prior to the inter-laboratory trial to confirm the fidelity and predictivity of the model. This provides benchmark data for others to compare the baseline output of their models when undertaking optimisation.
- Conduct an initial trial run to identify and resolve any teething issues prior to the formal inter-laboratory trial, as this will save both time and resources on unnecessary repeats and build confidence in the data produced. 'In-house' expertise workshops or training videos with troubleshooting can prove beneficial in the early stages.
- Include a known chemical positive alongside NMs known to give a positive and negative response, so that the expected toxicological response and classification can be clearly defined.
- Send all raw data generated to the host laboratory for uniformed analysis.

4. Conclusion

In conclusion, both the PHH microtissue and the 3D HepG2 spheroid models were shown to be robust and successfully transferable between academic and industrial laboratories. Once optimised, there was good concordance between the cytotoxicity, (pro-)inflammatory and genotoxicity responses observed with no significant difference in the data generated by each laboratory. This demonstrates the successful transfer of the SOPs across multiple laboratories, with strong reproducibility in hazard endpoint data subsequently generated. It will next be necessary to undertake validation trials to support the potential future use of these models for regulatory NM hazard assessment.

5. Materials and methods

5.1. In vitro models

5.1.1. Primary human multi-cellular liver microtissue model

The PHH model utilised was a commercially available, scaffold free, 3D InSight™ multi-donor human liver microtissue model (InSphero, Switzerland) composed of primary human hepatocytes (Lot#: IPHH18), primary human liver derived Kupffer cells and sinusoidal endothelial cells (Lot: IPHN15). The microtissues were maintained using the commercially provided InSightTM human liver maintenance medium (CS-07-305B-01, InSphero, Switzerland), in order to reduce variation amongst laboratories. Liver microtissues, in the 96-well plate format, were shipped to the recipient laboratories. On the day of arrival, a fresh culture medium (70 μL per well) exchange was performed, and the plates were incubated at 37 °C, 5% CO2, 95% humidity. Following 24 h incubation, the microtissue plates were exposed to the test agents.

5.1.2. 3D HepG2 spheroid model

The 3D HepG2 spheroid model was developed 'in-house' using the Human Caucasian Hepatocellular Carcinoma derived epithelial cell line, HepG2 (ATCC HB-8065), cultured in Dulbecco's Modified Eagle Medium (DMEM) with 4.5 g/L D-Glucose and L-Glutamine (GIBCO, Paisley, UK) supplemented with 10% Foetal Bovine Serum (FBS) and 1% Penicillin/Streptomycin antibiotic (GIBCO, Paisley, UK). A comprehensive SOP was generated following GIVIMP guidance, detailing how to construct the model, was distributed to all participating laboratories (Llewellyn et al., 2020). To form the 3D spheroid structure, HepG2 monolayers were trypsinised (0.05% trypsin/EDTA solution; GIBCO, Paisley, UK), a cell stock of 2.0 × 105 cells/mL was prepared, and the HepG2 cells cultured using the hanging drop method in a 96-well plate format (Llewellyn et al., 2020). In brief, 20 μL of the cell suspension (4000 HepG2 cells per 20 μL hanging drop) was pipetted onto the inverted side of a 96-well tissue culture plate lid (Nunc™ MicroWell™ 96-Well Microplates, Cat#: 167008, ThermoFisher Scientific, Denmark), before gently inverting the lid and placing back onto the 96-well plate filled with 100 μL of PBS (Conway et al., 2020). The plate was then placed in the incubator at 37 °C with 5% CO2 for three days before agarose transfer. Following 24 h incubation on agarose coated plates, the HepG2 spheroids were exposed to the test agents.

5.2. Experimental design

To assess the transferability and reproducibility of two *in vitro* liver models, PHH Microtissue Model and the 3D HepG2 Spheroid Model, the experimental design described in Table 2 was adopted for the inter-laboratory trial.

5.3. Chemical and engineered nanomaterial (NM) treatments

Full physico-chemical characterisation of the three NMs used in this study has been published previously (Llewellyn et al., n.d.; Keller et al., 2021; Yin et al., 2015; Kermanizadeh et al., 2013; JRC Nanomaterials

Table 2
Inter-laboratory trial experimental design to assess the transferability and reproducibility of two *in vitro* liver models; PHH Microtissue Model and the 3D HepG2 Spheroid Model.

Experimental design	Experiment 1	Experiment 2	
In Vitro liver model	Primary Multi-cellular Liver Microtissue Model	3D HepG2 Spheroid Model	
Exposure duration (hrs)	24	120	24
Treatment substance	TiO_2 and ZnO NM	$BaSO_4$ NM	B[*a*]P
Concentration	25.0 μg/mL 50.0 μg/mL	0.2 μg/mL 2.0 μg/mL	0.0–8.0 μM
Experimental controls	Untreated Media Control Triton-X Positive Control	Untreated Media Control Aflatoxin B1	Untreated Media Control
Biochemical endpoints	Cytotoxicity IL-8 (Pro-) inflammatory Response	IL-8 (Pro-) inflammatory Response	Cytotoxicity Genotoxicity
Laboratories involved	Laboratory A Laboratory B Laboratory C	Laboratory I Laboratory II Laboratory III	Laboratory I Laboratory IV

Repository | EU Science Hub, n.d).

5.3.1. Primary multi-cellular liver microtissue model

To assess the reproducibility of the primary coculture microtissue liver model for NM hazard assessment, acute (24 h) exposure to 25.0 μg/mL and 50.0 μg/mL of two NMs, TiO2 (NM-105, JRC Nanomaterials Repository, Italy) and ZnO (NM-111, JRC Nanomaterials Repository, Italy), were assessed in a simultaneous experiment involving the host laboratory and two other academic laboratories. The selection of the two doses were based on pilot work which investigated the acute toxicity of the selected NMs in the primary cell-based models. The decision for the selection of the higher concentrations was made to allow for the generation of detectable NM-induced toxicological outcomes that would allow for better understanding of the transferability and reproducibility of the data generated between the different laboratories. In addition, an untreated, media control and a positive control chemical of 1.0% Triton X-100 (Sigma Aldrich, UK) were also utilised.

5.3.2. 3D HepG2 spheroid model

For the HepG2 spheroid model, only one NM, BaSO4 (NM-220, Fraunhofer IME, Germany) was assessed using a prolonged five-day exposure to two, low-doses of 0.2 μg/mL and 2.0 μg/mL across. Both low-dose NM concentrations were selected, as 0.2 μg/mL of BaSO4 was previously shown to induce an elevated interleukin-8 (IL-8) response following a prolonged five-day exposure, whilst the higher concentration did not (Llewellyn et al., n.d.). To benchmark the 3D HepG2 spheroid model appropriately, an untreated, media only, negative control, and an assay positive chemical control of Tumor Necrosis Factor Alpha (TNF-α) protein (Cat# No: 2–35,076, BioTechne, UK) re-suspended in ddH2O according to manufacturer's instructions and diluted to a final working concentration of 0.25 μg/mL, were used in this study for the IL-8 ELISA Assay. The host laboratory and one other academic laboratory conducted the (pro-)inflammatory response inter-laboratory trial, whilst the host laboratory and a Contract Research Organization (CRO) conducted a genotoxicity inter-laboratory trial using the same 3D HepG2 spheroid model. For the genotoxicity study using the Cytokinesis-Block Micronucleus (CBMN) Assay, an untreated, media only negative control and a known liver carcinogen, B[*a*]P, were used to assess the inter-laboratory transferability and reproducibility. The HepG2 spheroids were exposed to concentrations of B[*a*]P ranging from 0.0 to 8.0 μM over a 24-h exposure period.

5.4. NM preparation and exposure regimes

Three NMs (TiO2 NM-105, ZnO NM-111, JRC Nanomaterials Repository, Belgium; BaSO4 NM-220, Fraunhofer IME, Germany) were stored as dry powders at room temperature until the day of exposure. NM stock solutions were prepared (2.56 mg/mL) and dispersed for 16 min in 0.05% Bovine Serum Albumin (BSA) using the probe sonication (Branson Sonifier 250, Ø 13 mm, 400 W output power, 20 kHz) method described by Jensen et al., 2014 (Alstrup Jensen, 2014). Working stocks of NMs were made fresh for each experiment. Following dispersion, NMs were diluted in the appropriate cell culture media to the desired concentrations required for either the PHH or HepG2 liver model.

5.4.1. Primary multi-cellular liver microtissue model

To perform the acute (24 h) NM exposures on the multicellular microtissue liver models, 70 μL of cell culture medium (8 wells per treatment) was aspirated per well and replaced with 50 μL of either media only, 1.0% Triton-X, or conditioned media containing either TiO2 and ZnO NMs at 25.0 μg/mL and 50.0 μg/mL. The microtissue plates were then incubated for 24 h at 37 °C and 5% CO2 before harvesting 50 μL of the cellular supernatant from each well. Supernatant from each treatment (8 wells in total; 400 μL) was pooled together for toxicological analysis.

5.4.2. 3D HepG2 spheroid model

To perform the prolonged (five-day) NM exposures using the HepG2 spheroid model, 50 μL of culture medium was removed from each well (16 wells per data point) and replaced with equal volumes of supplemented DMEM culture medium containing the exposure treatment; media only, 0.25 μg/mL TNF-α protein or conditioned media containing BaSO4 NMs at 0.2 μg/mL and 2.0 μg/mL. The HepG2 spheroids were then incubated for 5 days at 37 °C and 5% CO2, with media replenished on the third day by gently aspirating 50 μL of media from the surface of each well and replacing it with 50 μL of fresh media only. On the fifth day (120h), both the spheroids and the cellular supernatant were harvested simultaneously by aspirating 100 μL from each well and pooling together (16 wells per data point) into a falcon tube. The spheroid suspension was then centrifuged for 5 mins at 230 x*g*, prior to transferring the cell supernatant to a fresh tube. Cell supernatants were then stored at −70 °C until required for biochemical analysis.

Acute (24 h) chemical exposures for genotoxicity assessment using the HepG2 spheroid model were carried out as previously described by Shah et al. (Conway et al., 2020; Shah et al., 2018).

5.5. Adenylate kinase (AK) assay

As a measure of cytotoxicity, the cellular membrane integrity was evaluated using the ToxiLightTM Bioassay Kit (LT17–217, Lonza, UK) as per manufacturer's instructions. Pooled supernatant from the PHH microtissue plate was firstly centrifuged at 1000 x*g* for 2 mins, before 20 μL of cellular supernatant was aspirated and added to a 96-well white, flat bottom luminescence compatible plate (CLS3912-100EA, Sigma, UK). Following this, 80 μL of adenylate kinase (AK) detection buffer was added to all wells, and the plate incubated at room temperature for 5 min prior to measuring the luminescence using a standard plate-reading luminometer.

5.6. Interleukin 8 (IL-8) assay

Cytokine release was quantified by ELISA, using the cell supernatants described above in Section 2.3.1 and 2.3.2. DuoSet human antibody kits for IL-8 (DY208, DuoSet ELISA, R&D Systems) were used according to the manufacturer's instructions. The detection antibody was diluted as follows: IL-8: 0.1% BSA, 0.05% Tween 20 in Tris-buffered Saline (TBS), and incubated with the samples for 2 h at RT. The signal was developed using streptavidin horseradish-peroxidase and TMB Substrate Reagent A

& B (Cat# No. DY999, R&D Systems, UK). Absorbance was measured at 450 nm on an optical plate reader and the standard curve was plotted as 4-parameter logistic fit using the http://MyAssays.com software. Three biological replicates were assessed in triplicate.

5.7. Cytokinesis-block micronucleus (CBMN) assay

To assess cytotoxicity and genotoxicity following acute (24 h) exposure to B[*a*]P, the CBMN Assay was undertaken in conjunction with the Cytokinesis-Block Proliferation Index (CBPI) post-acute exposure. In short, following the harvest and removal of the cellular supernatant as described above, the remaining pooled liver spheroids were then trypsinised and a proportion of the cells taken to make slides for 20% Giemsa staining and manual cytotoxicity assessment. The remaining cells in suspension were then fixed for semi-automated micronucleus scoring, as previously described by Llewellyn et al., 2020 and Conway et al., 2020 (Llewellyn et al., 2020; Conway et al., 2020). A minimum of 1000 binucleated cells were counted per exposure dose per biological replicate ($n = 3$), using the principles established by Fenech et al. and in accordance with the OECD Test No. 487: *In Vitro* Mammalian Cell Micronucleus Test guidelines (Fenech, 2000; OECD, Test No. 487, 2016; Doak et al., 2012).

5.8. Statistics

Data and statistical analysis were performed using Prism 8, GraphPad Software, Inc. (USA). Shapiro-Wilk test was used to calculate normality for each data set, followed by a two-way ANOVA, with Tukey's multiple comparisons test to determine statistical significance (p value ≤ 0.05), unless otherwise stated. All experiments were performed with three biological replicates with mean data ± SEM presented.

Author contributions

SVL, AK, WM, VU, NRJ, UKS, KW, MN, SR were involved in data curation. SVL was responsible for formal analysis and writing original draft. GEC was responsible for writing reviewing and editing the manuscript. GJSJ, SHD and VS were responsible for conceptualization, funding acquisition and supervision.

Funding

This research was funded by European Union's Horizon 2020 research and innovation program for the PATROLS project, under grant agreement No.760813.

Data availability statement

In this section, please provide details regarding where data supporting reported results can be found, including links to publicly archived datasets analyzed or generated during the study. Please refer to suggested Data Availability Statements in section "MDPI Research Data Policies" at https://www.mdpi.com/ethics. If the study did not report any data, you might add "Not applicable" here.

Declaration of Competing Interest

The authors declare no competing interests and confirm the funders had no role in the design of the study; in the collection, analyses, or interpretation of data; in the writing of the manuscript, or in the decision to publish the results.

Acknowledgments

The authors would like to acknowledge the support and assistance provided by Keyan Wang (MiliiporeSigma) during data collection.

References

Alstrup Jensen, K., 2014. "The NANOGENOTOX Dispersion Protocol for NANoREG," Grant Agreement n° 2009 21 01. Accessed: Dec. 15, 2019. [Online]. Available: file:///C:/Users/Owner/Downloads/20140711+NANoREG+The+NANOGENOTOX+dispersion+protocol+for+NANoREG+V1+0.pdf.

Barosova, H., et al., Sep. 2021. Inter-laboratory variability of A549 epithelial cells grown under submerged and air-liquid interface conditions. Toxicol. in Vitro 75, 105178. https://doi.org/10.1016/J.TIV.2021.105178.

Bishara, N., Jan. 2012. The use of biomarkers for detection of early- and late-onset neonatal Sepsis. Hematol. Immunol. Infect. Dis. Neonatol. Quest. Controversies 303–315. https://doi.org/10.1016/B978-1-4377-2662-6.00018-3.

Bohmer, N., et al., Dec. 2018. Interference of engineered nanomaterials in flow cytometry: a case study. Colloids Surf. B: Biointerfaces 172, 635–645. https://doi.org/10.1016/J.COLSURFB.2018.09.021.

Conway, G.E., et al., 2020. Adaptation of the in vitro micronucleus assay for genotoxicity testing using 3D liver models supporting longer-term exposure durations. Mutagenesis. https://doi.org/10.1093/mutage/geaa018.

Desbaillets, I., Diserens, A.C., de Tribolet, N., Hamou, M.F., van Meir, E.G., Oct. 1997. Upregulation of interleukin 8 by oxygen-deprived cells in glioblastoma suggests a role in leukocyte activation, chemotaxis, and angiogenesis. J. Exp. Med. 186 (8), 1201–1212. https://doi.org/10.1084/jem.186.8.1201.

Doak, S.H., Manshian, B., Jenkins, G.J.S., Singh, N., Jun. 2012. In vitro genotoxicity testing strategy for nanomaterials and the adaptation of current OECD guidelines. Mutat. Res. Genet. Toxicol. Environ. Mutagen. 745 (1–2), 104–111. https://doi.org/10.1016/j.mrgentox.2011.09.013.

Elliott, J.T., et al., 2017. Toward achieving harmonization in a nano-cytotoxicity assay measurement through an interlaboratory comparison study. ALTEX 34 (2), 201–218. https://doi.org/10.14573/ALTEX.1605021.

Fenech, M., Nov. 2000. The in vitro micronucleus technique. Mutat. Res. 455 (1–2), 81–95. https://doi.org/10.1016/s0027-5107(00)00065-8.

van Grunsven, L.A., Nov. 2017. 3D in vitro models of liver fibrosis. Adv. Drug Deliv. Rev. 121, 133–146. https://doi.org/10.1016/j.addr.2017.07.004.

Hirsch, C., Schildknecht, S., 2019. In vitro research reproducibility: keeping up high standards. Front. Pharmacol. 10, 1484. https://doi.org/10.3389/FPHAR.2019.01484/BIBTEX.

Hirsch, C., Roesslein, M., Krug, H.F., Wick, P., Jul. 2011. Nanomaterial cell interactions: are current in vitro tests reliable? Nanomedicine (London) 6 (5), 837–847. https://doi.org/10.2217/NNM.11.88.

JRC Nanomaterials Repository | EU Science Hub. (accessed Feb. 16, 2022) https://ec.europa.eu/jrc/en/scientific-tool/jrc-nanomaterials-repository.

Keller, J.G., et al., 2021. Dosimetry in vitro–exploring the sensitivity of deposited dose predictions vs. affinity, polydispersity, freeze-thawing, and analytical methods. Nanotoxicology 15 (1), 21–34. https://doi.org/10.1080/17435390.2020.1836281.

Kermanizadeh, A., Gaiser, B.K., Hutchison, G.R., Stone, V., Jul. 2012. An in vitro liver model - assessing oxidative stress and genotoxicity following exposure of hepatocytes to a panel of engineered nanomaterials. Particle Fibre Toxicol. 9 (1), 28. https://doi.org/10.1186/1743-8977-9-28.

Kermanizadeh, A., et al., May 2013. "In vitro assessment of engineered nanomaterials using a hepatocyte cell line: cytotoxicity, pro-inflammatory cytokines and functional markers," doi:10.3109/17435390.2011.653416, vol. 7, no. 3, pp. 301–313. https://doi.org/10.3109/17435390.2011.653416.

Kermanizadeh, A., et al., Oct. 2014. Hepatic toxicology following single and multiple exposure of engineered nanomaterials utilising a novel primary human 3D liver microtissue model. Particle Fibre Toxicol. 11 (1), 56. https://doi.org/10.1186/s12989-014-0056-2.

Kermanizadeh, A., Balharry, D., Wallin, H., Loft, S., Møller, P., Nov. 26, 2015. Nanomaterial translocation-the biokinetics, tissue accumulation, toxicity and fate of materials in secondary organs-A review. Crit. Rev. Toxicol. 45 (10) https://doi.org/10.3109/10408444.2015.1058747. Taylor and Francis Ltd, pp. 837–872.

Kermanizadeh, A., Brown, D.M., Moritz, W., Stone, V., 2019, Dec. The importance of inter-individual Kupffer cell variability in the governance of hepatic toxicity in a 3D primary human liver microtissue model. Sci. Rep. 9 (1), 1–9. https://doi.org/10.1038/s41598-019-43870-8.

Kermanizadeh, A., et al., 2019, Nov. Assessment of nanomaterial-induced hepatotoxicity using a 3D human primary multi-cellular microtissue exposed repeatedly over 21 days - the suitability of the in vitro system as an in vivo surrogate. Particle Fibre Toxicol. 16 (1), 42. https://doi.org/10.1186/s12989-019-0326-0.

Lauschke, V.M., Hendriks, D.F.G., Bell, C.C., Andersson, T.B., Ingelman-Sundberg, M., Dec. 2016. Novel 3D culture Systems for Studies of human liver function and assessments of the hepatotoxicity of drugs and drug candidates. Chem. Res. Toxicol. 29 (12), 1936–1955. https://doi.org/10.1021/acs.chemrestox.6b00150.

Lauschke, V.M., Shafagh, R.Z., Hendriks, D.F.G., Ingelman-Sundberg, M., Jul. 2019. 3D primary hepatocyte culture Systems for Analyses of liver diseases, drug metabolism, and toxicity: emerging culture paradigms and applications. Biotechnol. J. 14 (7), 1800347. https://doi.org/10.1002/biot.201800347.

Llewellyn, S.V., et al., 2020. Advanced 3D liver models for in vitro genotoxicity testing following long-term nanomaterial exposure. J. Vis. Exp. 160, 2020. https://doi.org/10.3791/61141.

Llewellyn, S.V., et al., 2021, Jan. In Vitro Three-Dimensional Liver Models for Nanomaterial DNA Damage Assessment. In: Small, p. 2006055. https://doi.org/10.1002/smll.202006055.

Llewellyn, S.V., et al., 2021b. Simulating nanomaterial transformation in cascaded biological compartments to enhance the physiological relevance of in vitro dosing regimes: optional or required? Small. https://doi.org/10.1002/smll.202004630.

Llewellyn, S.v., et al., Dec. 2021. Understanding the impact of more realistic low-dose, prolonged engineered nanomaterial exposure on genotoxicity using 3D models of the human liver. J. Nanobiotechnol. 19 (1), 193. https://doi.org/10.1186/s12951-021-00938-w.

Niepel, M., et al., Jul. 2019. A multi-center study on the reproducibility of drug-response assays in mammalian cell lines. Cell Syst. 9 (1) https://doi.org/10.1016/J.CELS.2019.06.005, 35–48.e5.

OECD, 2018. Guidance Document on Good in Vitro Method Practices (GIVIMP). OECD Publishing.

OECD, Test No. 487, 2016. In Vitro Mammalian Cell Micronucleus Test. OECD. https://doi.org/10.1787/9789264264861-en.

Onakpoya, I.J., Heneghan, C.J., Aronson, J.K., Feb. 2016. Post-marketing withdrawal of 462 medicinal products because of adverse drug reactions: a systematic review of the world literature. BMC Med. 14 (1) https://doi.org/10.1186/S12916-016-0553-2.

PATROLS SOP Handbook. (accessed May 04, 2022) https://www.patrols-h2020.eu/publications/sops/index.php.

Petersen, E.J., et al., May 2020. Cause-and-effect analysis as a tool to improve the reproducibility of nanobioassays: four case studies. Chem. Res. Toxicol. 33 (5), 1039–1054. https://doi.org/10.1021/ACS.CHEMRESTOX.9B00165/SUPPL_FILE/TX9B00165_SI_001.PDF.

Piret, J.P., et al., Jun. 2017. Pan-European inter-laboratory studies on a panel of in vitro cytotoxicity and pro-inflammation assays for nanoparticles. Arch. Toxicol. 91 (6), 2315–2330. https://doi.org/10.1007/S00204-016-1897-2.

Shah, U.K., Mallia, J. de O., Singh, N., Chapman, K.E., Doak, S.H., Jenkins, G.J.S., 2018. Reprint of: a three-dimensional in vitro HepG2 cells liver spheroid model for genotoxicity studies. Mutat. Res. Genet. Toxicol. Environ. Mutagen. https://doi.org/10.1016/j.mrgentox.2018.06.020.

Siramshetty, V.B., Nickel, J., Omieczynski, C., Gohlke, B.O., Drwal, M.N., Preissner, R., 2016. Withdrawn—a resource for withdrawn and discontinued drugs. Nucleic Acids Res. 44 (Database issue), D1080. https://doi.org/10.1093/NAR/GKV1192.

Sison-Young, R.L., et al., Mar. 2017. A multicenter assessment of single-cell models aligned to standard measures of cell health for prediction of acute hepatotoxicity. Arch. Toxicol. 91 (3), 1385–1400. https://doi.org/10.1007/s00204-016-1745-4.

Sonna, L.A., Cullivan, M.L., Sheldon, H.K., Pratt, R.E., Lilly, C.M., 2003. Effect of hypoxia on gene expression by human hepatocytes (HepG2). Physiol. Genomics 12, 195–207. https://doi.org/10.1152/physiolgenomics.00104.2002.

The 3Rs | NC3Rs. (accessed Feb. 16, 2022) https://nc3rs.org.uk/who-we-are/3rs.

Trefts, E., Gannon, M., Wasserman, D.H., 2017. The liver. Curr. Biol. 27 (21), R1147. https://doi.org/10.1016/J.CUB.2017.09.019.

Xia, T., et al., Jun. 2013. Interlaboratory evaluation of in vitro cytotoxicity and inflammatory responses to engineered nanomaterials: the NIEHS Nano GO consortium. Environ. Health Perspect. 121 (6), 683–690. https://doi.org/10.1289/EHP.1306561.

Yin, H., et al., Feb. 2015. A comparative study of the physical and chemical properties of nano-sized ZnO particles from multiple batches of three commercial products. J. Nanopart. Res. 17 (2) https://doi.org/10.1007/s11051-014-2851-y.